ACS APPLIED MATERIALS & INTERFACES

www.acsami.org

Research Article

Heart Valves Cross-Linked with Erythrocyte Membrane Drug-Loaded Nanoparticles as a Biomimetic Strategy for Anti-coagulation, Anti-inflammation, Anti-calcification, and Endothelialization

Cheng Hu, Rifang Luo, and Yunbing Wang*

Cite This: *ACS Appl. Mater. Interfaces* 2020, 12, 41113–41126

Read Online

ACCESS | Metrics & More | Article Recommendations | Supporting Information

ABSTRACT: In recent years, valvular heart disease has become a serious disease threatening human life and is a major cause of death worldwide. However, the glutaraldehyde (GLU)-treated biological heart valves (BHVs) fail to meet all requirements of clinical application due to disadvantages such as valve thrombus, cytotoxicity, endothelialization difficulty, immune response, and calcification. Encouragingly, there are a large number of carboxyls as well as a few amino groups on the surface of GLU-treated BHVs that can be modified to enhance biocompatibility. Inspired by natural biological systems, we report a novel approach in which the heart valve was cross-linked with erythrocyte membrane biomimetic drug-loaded nanoparticles. Such modified heart valves not only preserved the structural integrity, stability, and mechanical properties of the GLU-treated BHVs but also greatly improved anti-coagulation, anti-inflammation, anti-calcification, and endothelialization. The *in vitro* results demonstrated that the modified heart valves had long-term anti-coagulation properties and enhanced endothelialization processes. The modified heart valves also showed good biocompatibility, including blood and cell biocompatibility. Most importantly, the modified heart valves reduced the TNF-α levels and increased IL-10 compared to GLU-treated BHVs. *In vivo* animal experiments also confirmed that the modified heart valves had an ultrastrong resistance to calcification after implantation in rats for 120 days. The mechanism of anti-calcification *in vivo* was mainly due to the controlled release of anti-inflammatory drugs that reduced the inflammatory response after valve implantation. In summary, this therapeutic approach based on BHVs cross-linking with erythrocyte membrane biomimetic nanoparticles sparks a novel design for valvular heart disease therapy.

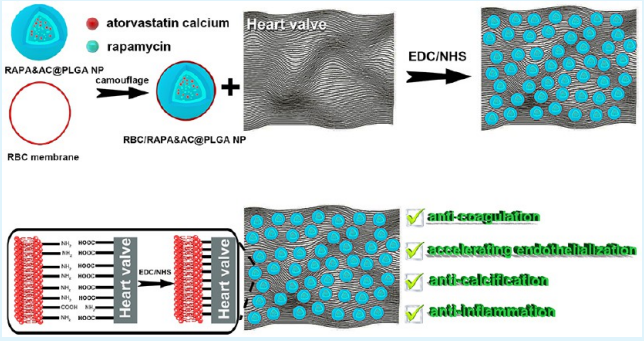

KEYWORDS: *biological heart valves, erythrocyte membrane, biomimetic drug-loaded nanoparticles, anti-calcification, inflammatory response*

1. INTRODUCTION

Valvular heart disease (VHD), including valve stenosis or reflux, affects more than 100 million people worldwide. It has become an increasingly serious problem, as the burden of degenerative valvular disease is increasing in the elderly population, and the incidence rate of rheumatic heart disease in developing countries remains high.[1,2] Currently, there is no effective medical treatment for cardiac valve dysfunction, mainly due to a lack of understanding of its pathophysiology.[3,4] Under grievous valvular dysfunction, replacing the damaged valve with an artificial valve (mainly including mechanical and biological valves) is the most effective solution.[5,6] It is expected that the number of patients requiring heart valve replacement will increase to over 850,000 by 2050.[7,8] Biological heart valves (BHVs) have been widely used,[9] and the proportion of patients with valvular disease receiving BHVs has increased each year, exceeding 80%.[10,11]

Nevertheless, using biomaterials from animals enhances the immunogenic response and increases the risk of transmitting diseases such as Creutzfeldt-Jakob disease, microorganisms, and retroviruses.[12,13] To resolve these issues, glutaraldehyde (GLU) may be employed as it is commonly used to treat biological tissue to obtain a fixed, nonliving, and nonresorbable matrix.[13] The latest clinical data indicate that interventional artificial heart valve products have a higher risk of subclinical valve thrombosis within 1 year after implantation, with an incidence of between 15% and 40%.[14,15] Although most valvular thrombosis is manifested as a valvular thickening and reduced valvular motility in the clinical setting, they may also result in valvular motility disorder and hydromechanical

Received: July 14, 2020
Accepted: August 24, 2020
Published: August 24, 2020

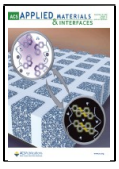

https://dx.doi.org/10.1021/acsami.0c12688
ACS Appl. Mater. Interfaces 2020, 12, 41113–41126

Scheme 1. Illustrations Displaying Preparation of Erythrocyte Membrane Biomimetic Drug-Loaded Nanoparticles and Mechanism of Cross-Linking with Heart Valves for Anti-coagulation/Accelerating Endothelialization Process/Anti-inflammation and Anti-calcification

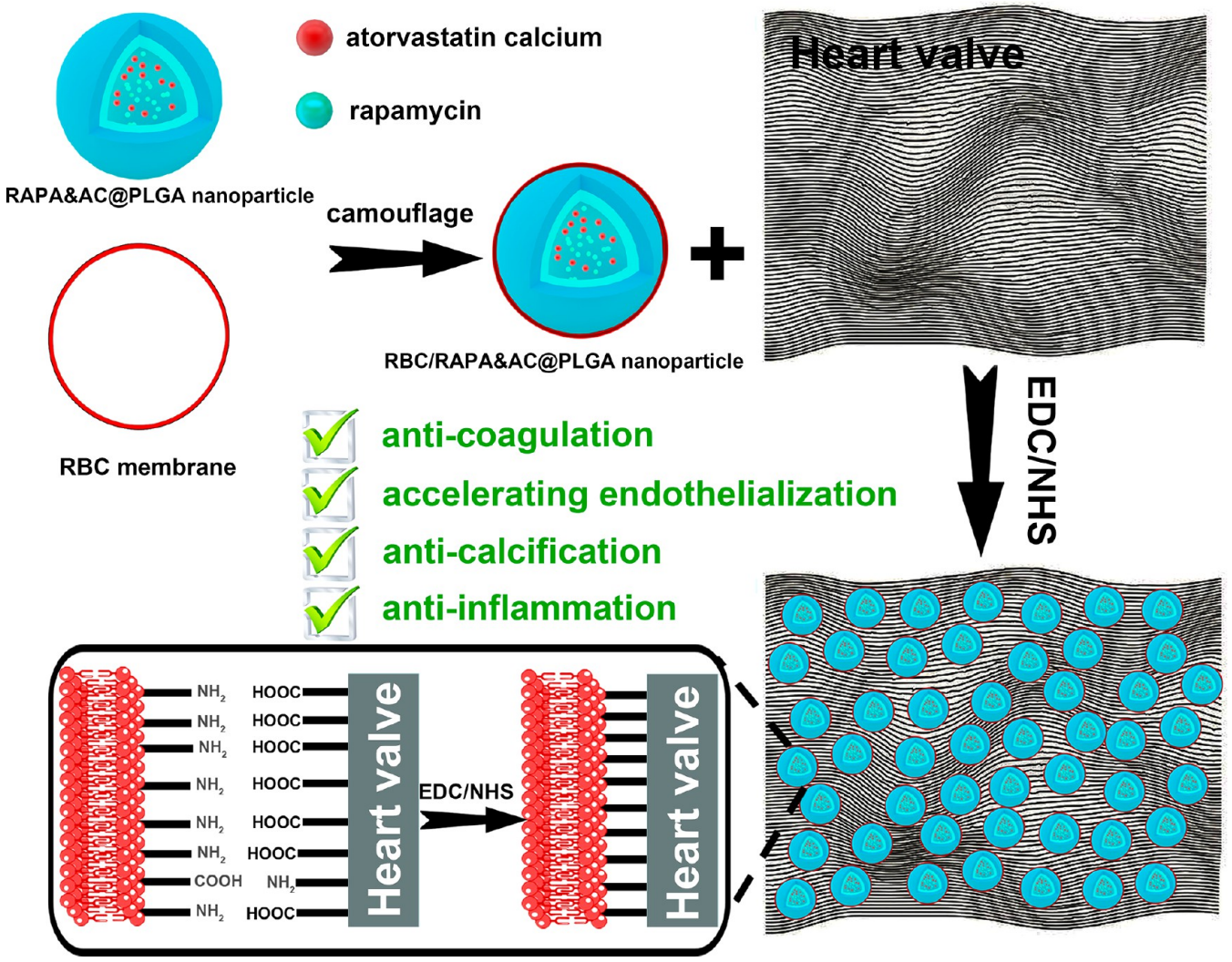

deterioration without intervention.[16] Furthermore, some patients may have clinical symptoms such as valvular stenosis, heart failure, fainting, and angina again. Meanwhile, valvular thrombosis is strongly correlated with the occurrence of complications, such as stroke and temporary cerebral ischemia, and it may further aggravate the occurrence of calcification.[17] This would result in opening and closing disorders of the valvular lobes and force the patient to have a second valve implantation operation.

At present, the transcatheter aortic valve replacement (TAVR) valve used in clinical practice is made from glutaraldehyde cross-linked porcine or bovine pericardium. These TAVR valves have been successfully used in elderly patients over 70 years of age. The patients tolerated the TAVR valves well for the rest of their lives. However, as a heteroplastic material, the valve lobe could promote the adhesion of platelets and local enrichment of clotting factors, thus causing valve lobe thrombosis.[18] GLU-treated BHVs could inhibit the adhesion and proliferation of endothelial cells due to the high toxicity of glutaraldehyde,[19] which is closely related to the aldehyde groups of the valve.[20] Still, the GLU-treated BHVs revealed the disadvantages such as immune response, valvular thrombosis, endothelialization difficulty, calcification seriousness, and a shorter life-span of the valve (generally only 10−15 years) due to altered mechanical properties and compromised functionality.[21,22] The short life span of the heart valves treated with glutaraldehyde is also detrimental for young patients who need much longer durability of the implanted valves. Therefore, it is the key point to improve the durability, safety, and life span of BHVs. Although some other valve modification methods have been reported to resolve these problems, the BHVs are still difficult to meet the requirements for clinical application.[23,24] Hence, the focus of our current research is seeking a new, nontoxic modification method to improve the endothelialization, anti-coagulation, anti-calcification, durability, life span, and other properties of biological valves that will minimize the side effects during and after valve replacement surgery.

Thanks to the advantages of nanomedicine delivery systems—such as prolonging drug half-life, strengthening site-specific targeting, reducing side effects and enhancing therapeutic efficacy—numerous nanotechnologies have emerged to sensitively diagnose or treat tumors,[25] microbial infections,[26] cardiovascular diseases[27] (including atheroscle-

https://dx.doi.org/10.1021/acsami.0c12688
ACS Appl. Mater. Interfaces 2020, 12, 41113−41126

rosis, VHD, and so on) and other diseases in recent years.[28] However, nanoparticles still have inherent shortcomings, including poor pharmacokinetics and pharmacodynamics, immunological response, systemic toxicity, rapid organism clearance, off-target protein adsorption, and nondegradability during long systemic circulation.[29] To address these above problems, researchers are developing novel drug carriers using the body's circulatory cells, including macrophages,[30] T cells,[31] neutrophils,[32] stem cells,[33] red blood cells,[34] and platelets,[35] to reduce reticuloendothelial system uptake, avoid immunological recognition, and decrease immune response and systemic toxicity.[36] Compared with conventional nanoparticles, cell membrane coated nanoparticles possess surface proteins of the membranes (composed of phospholipid bilayers, protein, cholesterol, and glycolipids), resulting in lower clearance rates *in vivo*, longer circulation time, and better biocompatibility and anti-coagulation properties.[37,38] But, a great challenge is how to combine cell membrane coated, drug-loaded nanoparticles with biological valves to achieve stable loading and controlled release of therapeutic drugs.

There are a large number of carboxyl groups and a few amino groups on the surface of GLU-treated BHVs available for modification. Cell membranes' surfaces also have many carboxyl and amino groups.[39] Inspired by this natural bioactivity, we hypothesized that the GLU-treated BHVs could cross-link with erythrocyte membrane biomimetic nanoparticles, leading to a large number of erythrocyte membrane biomimetic nanoparticles on the surface of the GLU-treated BHVs. In this work, we report a novel approach for the biomimetic modification of biological heart valves (Scheme 1). First of all, the erythrocyte/red blood cell (RBC) membrane biomimetic nanoparticles are cross-linked to the surface of the GLU-treated BHVs by the amidation reaction of the amino groups with carboxyl groups in the presence of 1-ethyl-3-(3-(dimethylamino)propyl)carbodiimide (EDC) and *N*-hydroxysuccinimide (NHS). These RBC membranes allow the biological valves to achieve the anti-coagulation/endothelialization and anti-calcification properties.[40] This strategy works by integrating the "natural" characteristics of the RBC membranes to make them anti-coagulant in blood circulation. Loading immunosuppressive agents and anti-inflammatory drugs to these RBC membrane coated nanoparticles could restrain the immune stress response more effectively after heart valve implantation and impart anti-calcification *via* inhibition of the inflammatory response. Rapamycin (RAPA) is considered as an effective immunosuppressive agent for immune rejection because of its specific pharmacological activity in targeting the mammalian target of rapamycin (mTOR) pathway.[41] Atorvastatin calcium (AC) has properties that can inhibit the inflammatory response.[42] Moreover, poly(lactic-*co*-glycolic) acid (PLGA), which has been approved by the U.S. Food and Drug Administration, works as a highly effective drug-loading material with biocompatibility and biodegradability.[43] Hence, the PLGA nanoparticles were loaded with RAPA and AC (RAPA&AC@PLGA). Subsequently, RBC vesicles were coated to the surface of RAPA&AC@PLGA nanoparticles to prepare the RBC-based nanocomplexes (RBC/RAPA&AC@PLGA). Finally, RBC/RAPA&AC@PLGA nanoparticles were cross-linked to the surface of the GLU-treated BHVs in the presence of EDC/NHS. In this study, we have shown that these biomimetic drug-loaded nanoparticles cross-linked on the surface of the porcine pericardial valve could enhance the anti-coagulant, endothelialization, and anti-calcification properties of porcine pericardial valves before and after implantation. Although it has been proved in previous studies that the lysed erythrocyte membrane can promote calcification,[44] the proposed biomimetic strategy of erythrocyte membrane in this work could effectively inhibit valve calcification, for the following reasons: (1) the "right-side-out" orientation of the erythrocyte membrane on the drug-loaded nanoparticles; (2) integrity of erythrocyte membrane structure and composition; (3) a very small amount of erythrocyte membrane bionic nanoparticles present on the valve surface; and (4) the controlled release of the anti-inflammatory drug atorvastatin calcium. More importantly, this strategy applies a biomimetic drug delivery system to porcine pericardial valve that holds considerable promise as a new generation treatment for safe and efficient valvular heart disease therapy. However, it must be emphasized that blood group matching is very important in future clinical use to avoid the hemolysis phenomenon after heart valve implantation. It is also better to select autologous (patients' own) RBCs or RBCs with the same blood type.

2. MATERIALS AND METHODS

2.1. Materials. Rapamycin, fluorescein diacetate (FDA), and atorvastatin calcium (AC) were obtained from Sigma-Aldrich. DiD (red) and DiO (green) dyes were added from Beyotime Institute of Biotechnology. Cell counting kit-8 was obtained from Dojindo Laboratories (Japan). Human umbilical vein endothelial cells (HUVECs) and macrophages were purchased from the Cellbank of the Chinese Academy of Sciences. All of the chemical reagents were obtained from Aladdin Reagent (Shanghai, China). Fresh glutaraldehyde-treated biological heart valves were kindly provided by Qiming Medical Appliances Co., Ltd. (Hangzhou, China), and the pericardium is from porcine origin.

2.2. Preparation of Red Blood Cell Vesicles. RBC vesicles were prepared according to the reported method in the previous reference.[34] Whole blood was obtained from Sprague−Dawley (SD) rats. First, the whole blood was centrifuged to remove serum at 4 °C (2000 rpm, 10 min). The red blood cells were washed with pH = 7.4 phosphate buffered saline (PBS, three times). Then, the red blood cells were resuspended in 0.25× PBS (pH = 7.4) containing EDTAK2 at 4 °C. After 30 min, the red blood cell solution was centrifuged at 4 °C (12000 rpm, 10 min); the pink precipitation was collected and stored at 4 °C.

2.3. Preparation of Drug-Loaded PLGA Nanoparticles (RAPA&AC@PLGA). PLGA (10 mg, MW 50000, 50:50), RAPA (1 mg), and AC (1 mg) were dissolved in 1 mL of dimethyl sulfoxide (DMSO). Subsequently, the mixture solution was dropwise added into 3 mL of water under gentle stirring. After 2 h, the solution was dialyzed using a dialysis bag (MWCO = 3500 Da) for 48 h. The fluorescence-labeled DiD@PLGA nanoparticles were prepared by loading 0.1 wt % DiD to PLGA nanoparticles.

2.4. Preparation of RBC Membrane Coating Nanoparticles. The RBC membrane coating nanoparticles were prepared by an extrusion method. First, RBC vesicles were prepared from 400 μL of whole blood. Subsequently, RBC vesicles were mixed with RAPA&AC@PLGA nanoparticles (2 mg/mL) and ultrasonicated (5 min). Then, the mixture solution was extruded with an Avanti mini-extruder (Avanti Polar Lipids, USA) through a polycarbonate porous membrane (100 nm) for 20 times. The RBC/PLGA, RBC/RAPA@PLGA, and RBC/AC@PLGA nanoparticles were prepared by the above method. Finally, the RBC membrane coating nanoparticles were stored at 4 °C.

2.5. Cross-Linking of Heart Valves and RBC Membrane Coating Nanoparticles. GLU-cross-linked heart valves were incubated with 0.1 M EDC and 0.1 M NHS for 3 h under vigorous stirring. After that, the RBC/PLGA (2 mg/mL), RBC/RAPA@PLGA, RBC/AC@PLGA, and RBC/RAPA&AC@PLGA (2 mg/mL)

https://dx.doi.org/10.1021/acsami.0c12688
ACS Appl. Mater. Interfaces 2020, 12, 41113−41126

nanoparticles solution was added for 2 days. After being washed with water 3 times, the heart valves cross-linked with erythrocyte membrane biomimetic drug-loaded nanoparticles were obtained. For RBC/RAPA@PLGA and RBC/AC@PLGA groups, to load the same amount of drugs as RBC/RAPA&AC@PLGA, the amounts of RBC/RAPA@PLGA and RBC/AC@PLGA were added according to the loading rate of each drug, respectively. Further, RBC/PLGA nanoparticles were also added to ensure that the number of nanoparticles was consistent in RBC/RAPA@PLGA and RBC/AC@PLGA groups. The number of nanoparticles on the heart valves was obtained from at least 10 different areas.

The initial weight (M0) of each lyophilized valve sample was measured and recorded. After all of the process of cross-linking the valve with the nanoparticle was completed, the modification valve was lyophilized and weighed (M1). The nanoparticle content was calculated with the following formula: nanoparticle content (%) = (M1 − M0)/M1 × 100. Each group consists of five parallel samples.

2.6. Characterization of Drug-Loaded Nanoparticles. The size distributions and ζ potentials of RAPA@PLGA, AC@PLGA, RAPA&AC@PLGA, RBC/RAPA@PLGA, RBC/AC@PLGA, and RBC/RAPA&AC@PLGA were detected by a Malvern Zetasizer Nano ZS unit (Malvern Zetasizer Nano-ZS90 apparatus, Malvern, U.K.) with a He−Ne laser (λ = 633 nm) at a scattering angle of 90° at 25 °C. Transmission electron microscope (TEM, Hitachi H-600, Japan) was used to observe the shapes of RAPA&AC@PLGA, and RBC/RAPA&AC@PLGA nanoparticles. The concentration of all samples for size distribution, ζ potential, and TEM detection was 1 mg/mL (H_2O is the solvent).

2.7. Characterization of Red Blood Cell Membrane Proteins. Polyacrylamide gel electrophoresis (SDS-PAGE) was utilized to characterize the membrane proteins. The protein samples of RBC vesicle and RBC/RAPA&AC@PLGA nanoparticles were separated on 12% SDS-PAGE gel and stained with the Coomassie blue. Western blot (WB) analysis was used to detect the CD47 protein.

Confirmation of Membrane Orientation. First, 1 mL of RAPA&AC@PLGA nanoparticles (1 mg mL^{-1}) and RBC/RAPA&AC@PLGA nanoparticles (1 mg mL^{-1}) were incubated with trypsin (5 μg) at 37 °C for 4 h. Then, the solutions were centrifuged (8000 rpm, 10 min) and the supernatant was collected to quantify glycoprotein using a rat glycoprotein enzyme-linked immunosorbent assay (ELISA) kit (Jiangsu Jingmei Biological Technology Co., Ltd.). There are five parallel samples for each group.

2.8. Differential Scanning Calorimetry and Attenuated Total Reflection Flourier Transformed Infrared Spectroscopy. Each heart valve sample (6−12 mg, n = 3) was cut and detected in an N_2 atmosphere using a differential scanning calorimetry (DSC) DSC 2920 instrument. There are three parallel samples for each group. Heart valve samples were equilibrated at 40 °C and heated at 10 °C/min up to 120 °C. The thermal shrinkage temperature was recorded as the maximum value of the endotherm peak. The specimens of GLU, RBC/RAPA@PLGA, RBC/AC@PLGA, and RBC/RAPA&AC@PLGA were freeze-dried and directly characterized by attenuated total reflection Fourier tranform infrared (ATR-FTIR; Spectrum One, Nicolet).

2.9. Enzymatic Stability of the Cross-Linked Heart Valves. The dried heart valve pieces were weighed (W0) and incubated in collagenase II (125 U mL^{-1}, pH 7.4) or elastase (30 U mL^{-1}, pH 7.4) tris buffer for 24 h, respectively. Then, the heart valves were washed with water 3 times and weighed (Wt) after being freeze-dried. The weight-loss percentage was counted by the following equation: percentage of weight loss (w/w, %) = (W0 − Wt)/W0 × 100%. There are six parallel samples for each group.

2.10. Tensile Test. Each heart valve sample was prepared into rectangles (40 × 8 mm^2), and the average thickness of samples was also detected by a thickness gauge at three different locations. Heart valves were installed into the fixture of the tensile testing equipment (Instron 5967) and tested. There are six parallel samples for each group.

2.11. Co-localization Experiment. Macrophages (RAW 264.7 cells) were inoculated and cultured for 24 h. RBC/DiD@PLGA nanoparticles (100 μg/mL) were added for 2 h. Then, the cells were washed with PBS (pH 7.4) three times and stained with DiO green (RBC membrane) and Hoechst 33342 (cell nucleus) for 30 min at room temperature. Then, the cells were imaged using confocal laser scanning microscopy (CLSM).

2.12. Loading of Drug and *In Vitro* Drug Release. RBC/RAPA@PLGA, RBC/AC@PLGA, and RBC/RAPA&AC@PLGA nanoparticles were dissolved in DMSO, respectively. The drug content was detected by high-performance liquid chromatography (HPLC). For the detection of AC, the mobile phase, and the detection wavelength were acetonitrile and water (40:60), and 241 nm, respectively. The methanol, acetonitrile, and water (67:15:18) as the mobile phase and 278 nm the detection wavelength for RAPA.

The drug-loading efficiency (DL) was counted by the previously reported method.[45]

A 1 mg/mL amount of RBC/RAPA&AC@PLGA nanoparticle solutions (n = 6) were added to dialysis bags (MWCO = 3500 Da) in PBS (pH 7.4). The 3 mL aliquot of PBS was extracted and 3 mL of fresh PBS (pH 7.4) was added at different times. The drug's cumulative released content was measured by the above method by HPLC.

2.13. Blood Compatibility Evaluation. For whole blood adhesion, heart valve samples were mounted into the flow chamber of the peristaltic pump and whole blood constantly flowed across the flow chamber for 45 min at 37 °C. For platelet adhesion, whole blood was centrifuged at 1600 rpm for 20 min to acquire the platelet-rich plasma. Different heart valve samples were treated with platelet-rich plasma at 37 °C under constant wobbling. The heart valves were washed with PBS 3 times after 2 h and fixed with 2.5% glutaraldehyde. Finally, the samples were surveyed by scanning electron microscope (SEM, S4800, Hitachi, Japan). The number of adherent red blood cells and platelets on the heart valves was obtained from at least six different areas.

Complement Activation. Complement activation studies were carried out by using plasma isolated by centrifugation from whole blood from the rat. Different heart valves samples (1 cm × 1 cm, n = 5) were treated with 500 μL of plasma at 37 °C for 1 h under constant wobbling. After 1 h incubation, the plasma was collected and measured by using a commercial C3a enzyme immunoassay kit (Jiangsu Jingmei Biological Technology Co., Ltd.).

Hemolysis Ratio of Heart Valves. Each heart valve sample was cut and suspended in 600 μL (containing 200 μL RBCs suspension) of PBS buffer for 2 h at 37 °C. H_2O and PBS were experimented with as positive control and negative control. After incubation for 2 h, the supernatant was centrifuged and 100 μL of supernatant was pipetted into a 96-well plate and the absorbance (541 nm) was detected with a microplate reader (Synergy H1, BioTek Instruments Inc.). The hemolysis ratio was calculated as follows: hemolysis ratio (%) = $(A_{sample} - A_{negative})/(A_{positive} - A_{negative}) \times 100$. There are six parallel samples for each group.

The platelet's poor plasma (PPP) was acquired by centrifuging whole blood (3000 rpm, 15 min). Each heart valve sample was treated with PPP at 37 °C for 30 min under constant wobbling. Then, samples were detected by an automatic coagulation analyzer (Sysmex CS5100, Japan). There are six parallel samples for each group.

2.14. HUVECs Culture. To prepare the diluted extraction of the heart valve samples, the valve samples were immersed in a complete cell medium after radiation disinfection with a concentration of 0.2 g/mL and extracted for 72 h. The HUVECs were incubated at 37 °C under 5% CO_2. Heart valve samples (six parallel samples in each group) were disinfected by 75% ethanol solution for 24 h. Then heart valve samples were washed with PBS and placed in 96-well plate. A 100 μL aliquot of HUVECs cell suspension was seeded at a density of 2 × 10^4 cells per well. At 1 day and 3 days, 100 μL of medium (10% CCK-8 reagent) was added and cultured for 2 h. And the absorbance (450 nm) was detected with a microplate reader (Synergy H1, BioTek Instruments Inc.).

For cell FDA staining, cells were immersed in FDA for 10 min. The cell morphology was imaged by a fluorescence microscope (Leica DMI 4000, Germany) at 1 day and 3 days.

https://dx.doi.org/10.1021/acsami.0c12688
ACS Appl. Mater. Interfaces 2020, 12, 41113−41126

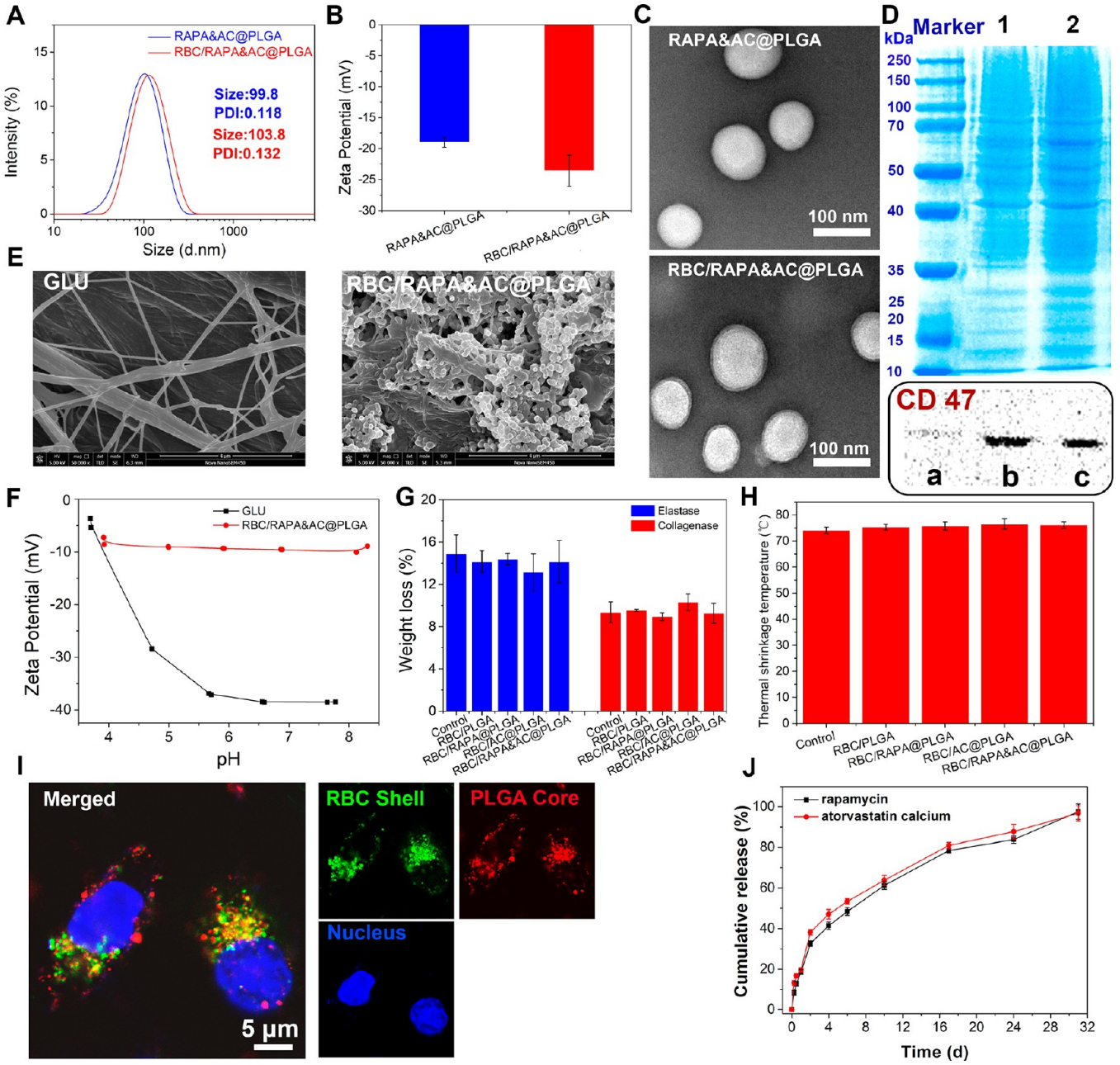

Figure 1. (A) Size and (B) ζ potential of RAPA&AC@PLGA and RBC/RAPA&AC@PLGA (n = 3). (C) TEM images of RAPA&AC@PLGA and RBC/RAPA&AC@PLGA (scale bar = 100 nm). (D) Proteins of RBC vesicles (group 1) and RBC/RAPA&AC@PLGA nanoparticles (group 2) characterized by SDS-PAGE (top); Western blot analysis of CD47 in RAPA&AC@PLGA nanoparticles (group a), RBC vesicles (group b), and RBC/RAPA&AC@PLGA nanoparticles (group c) (bottom). (E) SEM images of heart valves treated with or without RBC/RAPA&AC@PLGA (scale bar = 4 μm). (F) ζ potential of GLU-treated or RBC/RAPA&AC@PLGA-treated heart valves at different pH values. (G) Weight-loss ratios (n = 6) of GLU, RBC/PLGA, RBC/RAPA@PLGA, RBC/AC@PLGA, and RBC/RAPA&AC@PLGA-treated heart valves after treatment with collagenase and elastase for 24 h at 37 °C (n = 6) (GLU-treated heart valve selected as a control group). (H) Thermal shrinkage temperatures of GLU, RBC/PLGA, RBC/RAPA@PLGA, RBC/AC@PLGA, and RBC/RAPA&AC@PLGA-treated heart valves (n = 3) (GLU-treated heart valve selected as a control group). (I) CLSM images for fluorescence co-location of macrophage treated with RBC/DiD@PLGA nanoparticles for 2 h, including the nucleus channel (blue), RBC shell (green) channel, nanoparticles core (red) channel, and overlay of previous (scale bar = 5 μm). (J) Rapamycin and atorvastatin calcium cumulative release at different time points (n = 3).

2.15. Cell Viability of RAW 264.7 Cells *In Vitro*. Macrophages were seeded in a 96-well plate (10^4 cells per well). After 12 h, the cells were pretreated with lipopolysaccharide (LPS, 10 μg/mL) for 2 h and incubated with diluted extraction of the heart valve samples for another 24 and 72 h. The cell viability was measured by CCK-8 assay and calculated according to the methods reported in previous literature.[46]

2.16. ELISA Assay. Macrophages were seeded into 6-well plates (5×10^6 cells per well). After 24 h, the media was replaced with DMEM media containing LPS (10 μg/mL) for 2 h. Next, the macrophages were treated with 2 mL of diluted extraction of the different valve samples for 72 h, respectively. Finally, the supernatants were measured by ELISA assay following the manufacturer's instructions.

https://dx.doi.org/10.1021/acsami.0c12688
ACS Appl. Mater. Interfaces 2020, 12, 41113−41126

2.17. Western Blot. Macrophages, after incubation with 2 mL diluted extraction of the different valve samples for 72 h, were lysed at 4 °C for 30 min. Then samples were centrifuged at 12000 rpm for 20 min. The BCA protein assay kit (Beyotime) was used to detect protein concentration. Then cell lysates containing equivalent amounts of protein were separated by SDS-PAGE and electro-transferred onto poly(vinylidene fluoride) (PVDF) membranes. After being blocked with 5% (w/v) skim milk powder in tri-*sec*-buffered-saline with Tween-20 (TBST) for 1 h at 37 °C, the PVDF membranes were incubated overnight with TNF-α antibody (1:500 of dilution) or IL-10 antibody (1:1000 of dilution) at 4 °C with gentle shaking. Then membranes were washed and incubated secondary antibody (1:5000 of dilution) for 1 h at room temperature. Finally, the membranes were visualized with ECL reagent (Thermo Scientific) and imaged by the ChemiDoc-XRS imaging system (Bio-Rad).

2.18. Immunofluorescence Staining. Macrophages were pre-treated with LPS (10 μg/mL) for 2 h. Next, the macrophages were treated with 2 mL diluted extraction of the heart valves. After 72 h, the cells were rinsed with PBS and fixed with 4% paraformaldehyde (37 °C, 15 min). After being washed with PBS three times, the macrophages were treated with mouse anti-TNF-α (1:100 dilution) or anti-IL-10 antibodies (1:100 dilution) overnight at 4 °C. Then macrophages were treated with FITC-labeled secondary antibody for 1.5 h. Finally, macrophages were incubated with Hoechst 33342 at 37 °C for 20 min. Finally, the cells were imaged using CLSM.

2.19. Implantation and Explantation of Heart Valves. All animal experiments have been authorized by the Medical Ethics Committee of Sichuan University. There are six parallel samples in each group. Heart valves were disinfected with 75% ethanol overnight and washed with PBS (pH 7.4). Sprague−Dawley (SD) rats were anesthetized using sodium pentobarbital. On the back of SD rats, a longitudinal surgical incision was made. Heart valve samples for each group were implanted subcutaneously in male SD rats (150 ± 10 g). Then rats were euthanized at 7, 30, 60, and 120 days; the surrounding tissues containing heart valve samples were extracted and fixed with 4% paraformaldehyde for 24 h.

2.20. Histological Analysis. For histological analysis, the H&E of tissue sections was used to examine the biocompatibility of different heart valve samples *in vivo*. Calcium deposition was stained by alizarin red. Anti-rat IL-10 antibody and anti-rat TNF-α antibody were utilized to evaluate the inflammation of different heart valve samples in the body. Slide scanner (MIRAX Desk, Carl Zeiss Microimaging GmbH, Germany) and Image-Pro Plus software were used to observe the images and quantify the immunopositive cells, respectively.

2.21. Quantitative Analysis of Calcium. Explanted heart valve samples (n = 6) were freeze-dried and weighed. Then heart valve samples were dissolved with 6 M HCl solution at 100 °C for 12 h. The calcium content was detected with ICP-OES by Ceshigo Research Service, www.ceshigo.com.

3. RESULTS AND DISCUSSION

First, we synthesized a RBC-like drug delivery platform by fusing RBC membranes onto the surface of PLGA nanoparticles. Figure 1A showed the size of the drug-loaded nanoparticles after coating with RBC vesicles increased from 99 to 103 nm, indicating that the RBC membrane was successfully attached onto the surface of RAPA&AC@PLGA nanoparticles.[34] The results in Supporting Information Figure S1 described a similar consequence. In addition, ζ potential (Figure 1B and Figure S2) displayed that RAPA&AC@PLGA (−18.7 mV) has a slight decrease in ζ potential after the cell membrane coating (RBC/RAPA&AC@PLGA, −22.7 mV). For RBC/RAPA&AC@PLGA nanoparticles, the drug loadings of RAPA and AC were 3.04% and 5.43%, respectively (Table 1). From the SEM images in Figure 1C, the RBC membrane was observed on the surface of RAPA&AC@PLGA nanoparticles, further showing successful coating.[47] And the nanoparticles before and after coating were both monodispersed. The SDS-PAGE results in Figure 1D (top) illustrated that the protein bands of RBC vesicles and RBC/RAPA&AC@PLGA were highly consistent, suggesting that none of the membrane proteins were destroyed throughout the fabrication. CD47 has been identified on the RBC surface as a self-marker that inhibits macrophage phagocytosis.[48] It plays an important role in bypassing the immune recognition process, improving the *in vivo* circulation time and biocompatibility.[49] The Western blot results in Figure 1D (bottom) indicated that this CD47 protein appeared on the RBC/RAPA&AC@PLGA nanoparticles. As shown in Figure S3, compared with the equivalent amount in RBC vesicles, the average content of glycoprotein on RBC/RAPA&AC@PLGA nanoparticles was approximately 92.2%. This quantification indicated that glycoproteins were retained on the outside surface of the RBC/RAPA&AC@PLGA nanoparticles, demonstrating the "right-side-out" orientation of the RBC membrane on the drug-loaded nanoparticles.[34] SEM was used to verify whether the erythrocyte membrane biomimetic drug-loaded nanoparticles could be successfully cross-linked to the heart valves surface. The SEM images in Figure 1E and Figure S4 indicated that these biomimetic nanoparticles were successfully cross-linked with heart valves, and that large numbers of nanoparticles were observed on the heart valve surface.[50] The number of nanoparticles on the surfaces of valve samples was also quantified in Figure S5, showing a grafting density of approximately 45 nanoparticles/μm^2. The weight change after incorporating these biomimetic nanoparticles onto the heart valve samples was shown in Figure S6. The results suggested that the nanoparticle content after the cross-linking was about 0.9%. To further demonstrate that the biomimetic drug-loaded nanoparticles were successfully cross-linked onto the heart valve surface, ATR-FTIR spectrum was used to identify the characteristic peak of the amide bond (Figure S7).[50] The amide-linked C═O stretching vibrations resulted in a newly appeared peak at 1690 cm^{-1}, and the telescopic vibration absorption peak of the carboxyl group was broad and weak at 3000−3280 cm^{-1} in the RBC/RAPA&AC@PLGA group compared with a sharp absorption peak of the carboxyl group in GLU group. Next, the surface ζ potential of the heart valves was studied at different pH values. According to the data in Figure 1F, the surface ζ potential of the GLU group decreased from −5.4 to −38.5 mV with a corresponding increase in pH value from 3.7 to 7.6 and the surface ζ potential of the GLU group was approximately −37 mV when the pH was 7.4. In contrast, the surface ζ potential of the heart valve group modified with RBC/RAPA&AC@PLGA nanoparticles was very stable (from −8.6 to −10.0 mV) at pH values ranging from 3.9 to 8.1, the surface ζ potential was about −8 mV when the pH was 7.4. The weight-loss ratio of heart valves after being treated with collagenase was used to assess the protection of collagen.[21] GLU, RBC/PLGA, RBC/RAPA@PLGA, RBC/AC@PLGA, and RBC/RAPA&AC@

Table 1. Drug-Loading Efficiency of the RBC/RAPA@PLGA, RBC/AC@PLGA, and RBC/RAPA&AC@PLGA (n = 3)

sample ID	RAPA-loading efficiency (%)	AC-loading efficiency (%)
RBC/RAPA@PLGA	7.54 ± 0.98	N/A
RBC/AC@PLGA	N/A	9.41 ± 0.75
RBC/RAPA&AC@PLGA	3.04 ± 0.21	5.43 ± 0.65

https://dx.doi.org/10.1021/acsami.0c12688
ACS Appl. Mater. Interfaces 2020, 12, 41113−41126

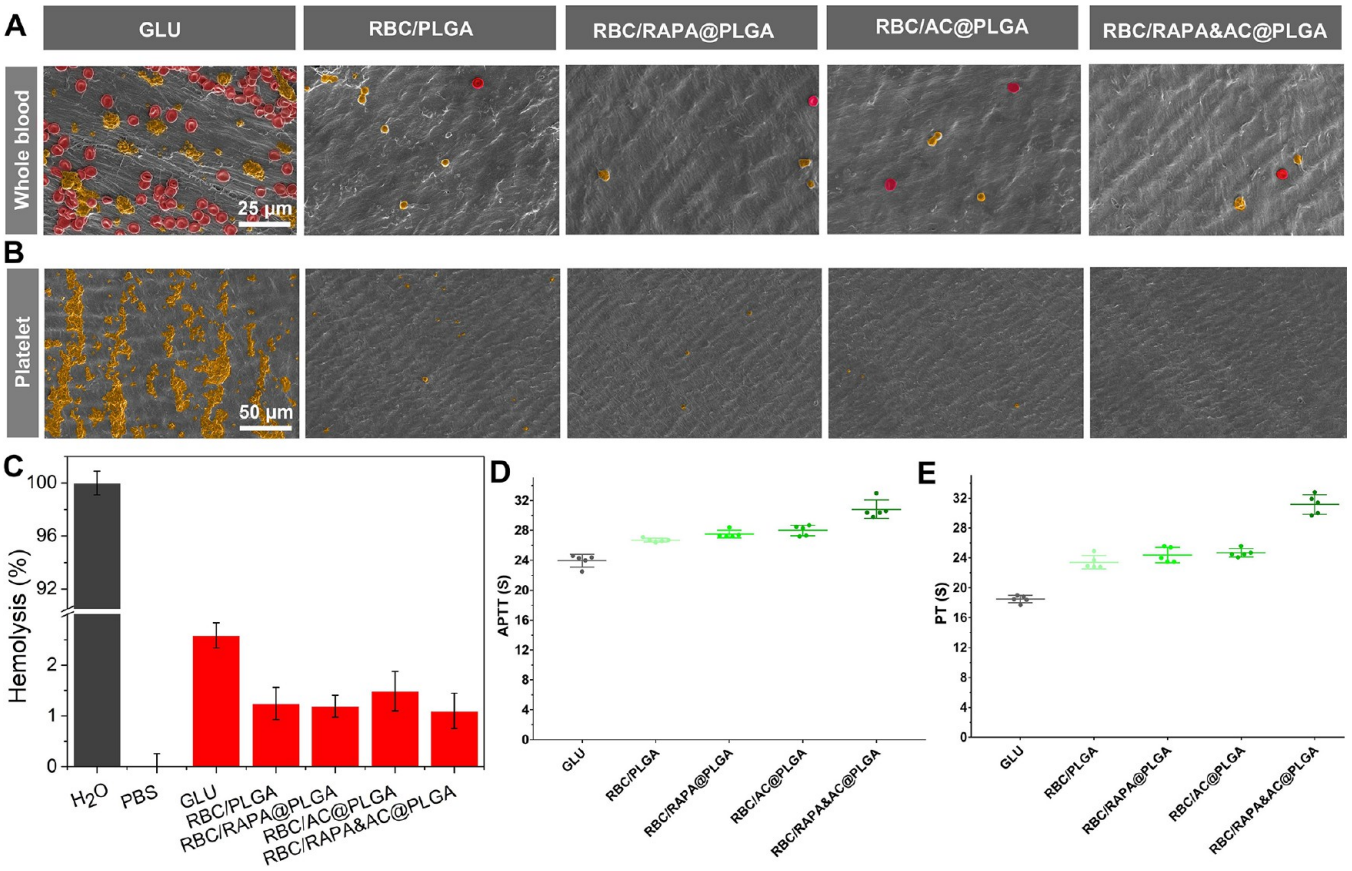

Figure 2. (A) SEM of heart valves on different samples after treatment with whole blood. The red blood cells were marked as red, and the platelets were marked as yellow. (B) SEM of heart valves on different samples after treatment with platelets. The platelets were marked as yellow. (C) Quantitative results for the hemolysis effect for the different samples. (D) APTT for different heart valve samples after treatment with PPP. (E) PT for different heart valve samples after treatment with PPP.

PLGA groups (Figure 1G) emerged with weight-loss ratios of 9.37, 9.69, 9.19, 8.89, and 9.72%, respectively. This result did not show large differences in the weight-loss percentages compared to the GLU group, demonstrating that the nanoparticle modification did not change the collagen stability of the heart valves. Further, when the GLU, RBC/PLGA, RBC/RAPA@PLGA, RBC/AC@PLGA, and RBC/RAPA&AC@PLGA groups were treated with elastase, similar weight-loss ratios (RBC/PLGA, 13.61%; RBC/RAPA@PLGA, 13.98%; RBC/AC@PLGA, 13.65%; and RBC/RAPA&AC@PLGA, 12.60%) did not significantly differ from that of the GLU group (14.74%), indicating that the nanoparticles did not change the elastin protection of the heart valves (Figure 1G). Differential scanning calorimetry (DSC) was used to detect the thermal shrinkage temperature of the heart valves and determine whether or not the modification of the drug-loaded nanoparticles could enhance the heart valve collagen stability.[9] This result, shown in Figure 1H, demonstrated that the thermal shrinkage temperatures of heart valves before and after being modified by the nanoparticles was similar to that of the GLU group (about 75 °C). Additionally, the stress−strain curve was used to evaluate the mechanical property of the heart valves.[24] The results in Figure S9 showed that the stress−strain curves of the heart valves after being cross-linked with biomimetic drug-loaded nanoparticles were similar to that of the GLU group, indicating that the surface modification process did not significantly change the mechanical property of the heart valves. The fluorescent images (Figure 1I) showed that most of the nanoparticles (red) co-localized with the RBC membrane shell (green), suggesting the structure of the nanoparticles was still intact after cell internalization. Finally, the release kinetics of RAPA and AC from RBC/RAPA&AC@PLGA nanoparticles was researched in PBS (pH 7.4) solution. The results in Figure 1J revealed that the cumulative release of both drugs was controlled release in 31 days. After 4 days of incubation, 41.43% RAPA was released from RBC/RAPA&AC@PLGA nanoparticles, while 47.1% AC was released from the RBC/RAPA&AC@PLGA nanoparticles. At 31 days, 97.5% RAPA and 96.8% AC were released, respectively.

Furthermore, we first evaluated whether the EDC/NHS treating process would affect the cytocompatibility of the heart valves before evaluating other biological properties. As shown in Figure S10, in the GLU valves treated by the EDC/NHS only group, the viability of L929 cells was similar to that of the GLU-treated-valves group. The results suggested that the cytotoxicity of the GLU-treated valves was not significantly affected after treatment by EDC/NHS only, and similar cell viability results were also found in the HUVECs in Figure S11. Meanwhile, after cultivating with the extraction of the bionic modified heart valves for 24 and 72 h, the viability of L929 cells and HUVECs in all groups was more than 90%, suggesting that the heart valves were nontoxic and showed good biocompatibility to L929 cells and HUVECs after modifying with RBC membranes' biomimetic nanoparticles. To sum up, the GLU-treated valves after treatment by EDC/NHS only would not affect their cytocompatibility.

https://dx.doi.org/10.1021/acsami.0c12688
ACS Appl. Mater. Interfaces 2020, 12, 41113−41126

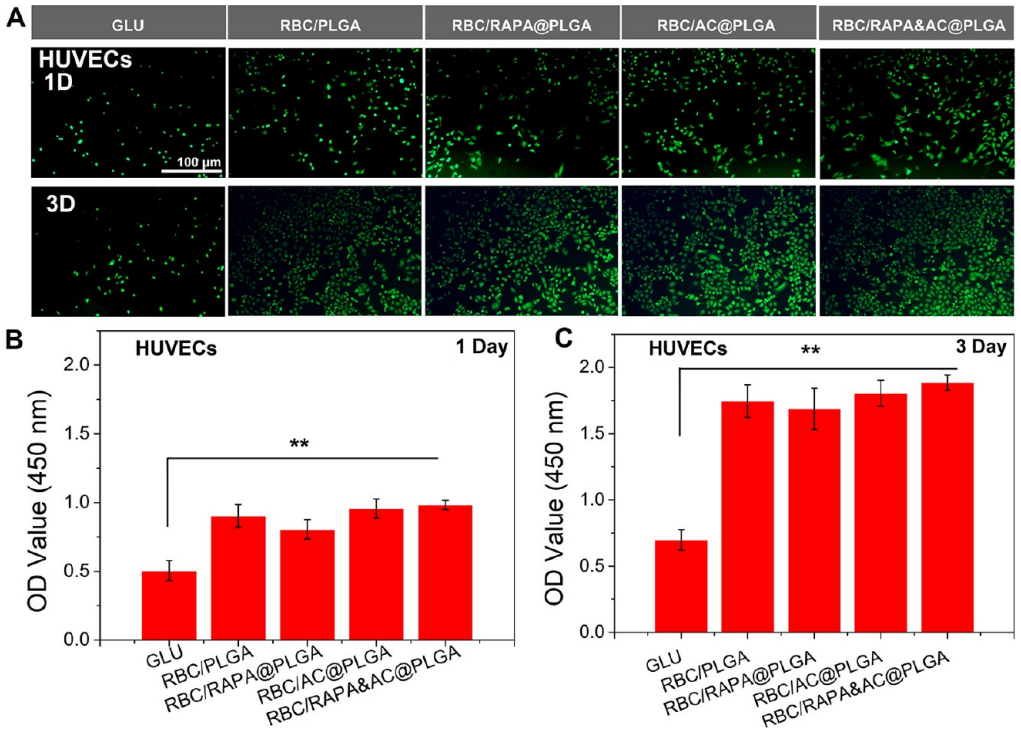

Figure 3. (A) Live staining of HUVECs on different heart valve samples at 1 day and 3 days (scale bar = 100 μm). (B) Cell viability of HUVECs on different heart valve samples at 1 day (mean ± SD; $n = 6$; **, $P < 0.001$). (C) Cell viability of HUVECs on different heart valve samples at 3 days (mean ± SD; $n = 6$; **, $P < 0.001$).

Next, the blood compatibility and anti-coagulant properties of heart valves before and after modification by nanoparticles were investigated. The results for adhesion of whole blood on different heart valve samples were shown in Figure 2A. The number of adhered things (RBC, platelet, and so on) on the GLU group was greater than that on the other heart valve groups. In particular, the results in Figure S12 showed that the number of adhered things on the surface of the GLU group is over 13 times more than that of the RBC/RAPA&AC@PLGA group. These results indicated that modifying heart valves with RBC-coated, drug-loaded nanoparticles effectively inhibited blood adherence and promoted better blood compatibility. Platelet activation and adhesion was also investigated. The results in Figure 2B showed that many platelets adhered to the GLU group. The morphology of the platelets was irregular and protruded with a large number of pseudopodia, suggesting that the adhered platelets were activated. However, only a few platelets were found on the surfaces of heart valve samples from the other groups. The sizes of the platelets were rounder, suggesting less platelet activation.[51] The numbers of platelets adsorbed onto the surfaces of valves were also counted. The results in Figure S13 showed that the number of platelets in the RBC/RAPA&AC@PLGA group was 752 per mm^2; it is significantly less than the 15620 per mm^2 found in the GLU group. These results suggested that the heart valves showed better anti-coagulant properties than the GLU group after bionic nanoparticle modification. These benefits were caused by the RBC membrane coated nanoparticles as well as the cross-linking and consumption of carboxyl and amino groups on the surface after the valve modification. When blood comes into contact with foreign materials, the complement system of the host defense system would activate.[52] In the process of activation, complement component C3 is cleaved into C3a and C3b. And the level of complement activation was indicated by the concentration of C3a in plasma. Here, the concentration of C3a in plasma was monitored by using a C3a enzyme immunoassay kit. Figure S14 showed the concentrations of C3a in the plasma after treatment of different heart valve samples. The result indicated that RBC membrane modified valves caused significantly weaker complement activation when compared to the GLU-treated valves (51.6 ng/mL). The effect was significantly decreased in RBC/RAPA@PLGA (23.2 ng/mL) and RBC/RAPA&AC@PLGA groups (23.0 ng/mL) due to the controlled release of RAPA. The concentration of the RBC/RAPA&AC@PLGA group was very close to that of the control group (20.9 ng/mL), indicating that the complement system was not activated after biomimetic nanoparticle modified valves implantation. On the basis of the result, the modification strategy (the patient's cell membrane and the immunosuppressive-loaded nanoparticles) will greatly suppress the complement activation of the xenogenic graft material when the valve is transplanted into the human body. However, considering the differences between species and the application of these biomimetic-modified valves in the human body, the evaluation of the complement activation response after valve implantation has not been very comprehensive. The galactose, a 1,3-galactose (Gal) antigen, is widely presented in bioprosthetic heart valves, especially in porcine and bovine tissues.[53,54] Most importantly, it is also retained in currently used commercial BHVs.[55] And different from protein antigens, Gal remains immunogenic after fixation.[54] Thus, in the next step, we will focus on evaluating whether the modified heart valves can reduce the complement activation response induced by Gal antigen of xenogenic tissues after implantation. Given that heart valves are blood-contacting medical devices, hemolysis is very crucial.[56] The hemolysis ratios of the RBC/RAPA&AC@PLGA group and GLU group were 1.09% and 2.58%, respectively (Figure 2C). The hemolysis ratios that

https://dx.doi.org/10.1021/acsami.0c12688
ACS Appl. Mater. Interfaces 2020, 12, 41113−41126

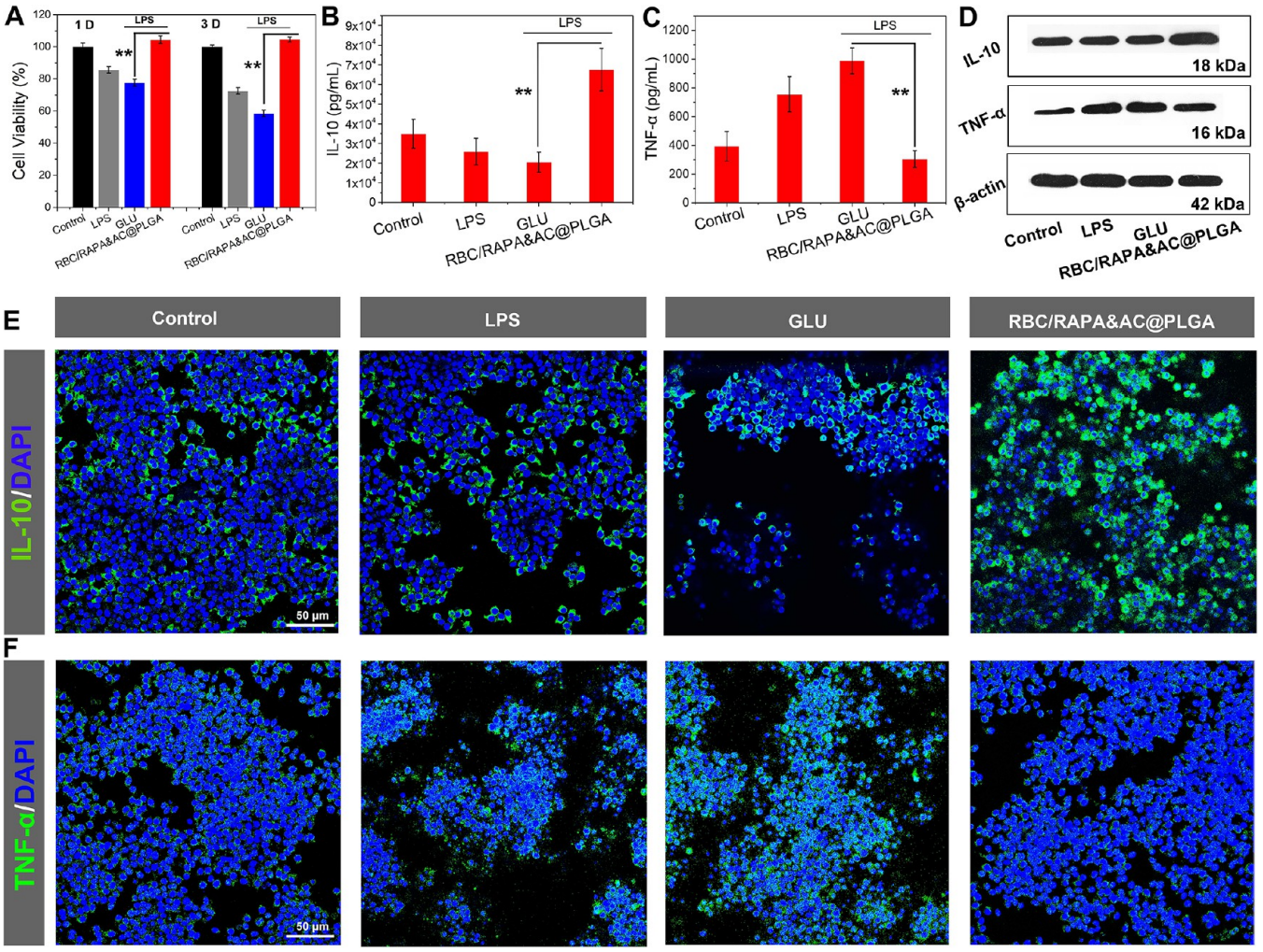

Figure 4. (A) Cell viability of macrophages when contacting with leaching solution of different heart valves for 1 day and 3 days (mean ± SD; n = 6; **,P < 0.001). Macrophage was pretreated with LPS for 2 h. (B) IL-10 in the supernatant detected by enzyme-linked immunosorbent assay (ELISA) (mean ± SD; n = 6; **, P < 0.001). (C) TNF-α in the supernatant detected by ELISA assay (mean ± SD; n = 6; **, P < 0.001). (D) Expression levels of IL-10 and TNF-α measured by using immunoblot analysis (β-actin selected as a control group). (E) Immunofluorescence staining of IL-10 for macrophages. (F) Immunofluorescence staining of TNF-α for macrophages. All scale bars = 50 μm.

were less than 3% were considered as receivable. Furthermore, the activated partial thromboplastin time (APTT) and prothrombin time (PT) were also utilized to assess the heart valve anti-coagulation properties.[57] The result shown in Figure 2D indicated that the APTT of the RBC/RAPA&AC@PLGA group (31.0 s) was slower than the GLU group (23.9 s). A similar phenomenon was also found in Figure 2E; the PTs of RBC/RAPA&AC@PLGA group and GLU group were 31.2 and 18.5 s, respectively. From what has been discussed above, after modification the RBC-coated, drug-loaded nanoparticles, heart valves should have less blood adhered and activated platelets. Taken together, these findings suggest that modifying the heart valves with RBC-coated, drug-loaded nanoparticles is a very good strategy for potential long-term anti-coagulation properties and good blood compatibility.

Endothelialization on heart valves is critical to maintaining mechanical stability during long-term usages after implantation. Human umbilical vein endothelial cells were utilized to investigate whether modified heart valves could enhance HUVECs adhesion, growth, and proliferation.[20] As shown in Figure 3A, the fluorescein diacetate staining was utilized to evaluate the morphology and quantity of HUVECs. The results in Figure 3A indicated that few HUVECs attached and grew in the GLU group after incubating for 1 day due to the cytotoxicity of GLU. However, more cells were observed in the RBC/PLGA, RBC/RAPA@PLGA, RBC/AC@PLGA, and RBC/RAPA&AC@PLGA groups at 1 day (Figure 3A). After culturing for 3 days, most cells could be found on the RBC/RAPA&AC@PLGA group surface compared with other groups. And CCK-8 results for 1 day and 3 days were shown in Figure 3B,C. The CCK-8 quantitative results exhibited the lower absorbance for the GLU group and the higher absorbance for the RBC/RAPA&AC@PLGA group at 1 day and 3 days, respectively. These results showed that the cytocompatibility and endothelialization process were enhanced after the heart valve was modified with the RBC-coated drug-loaded nanoparticles. The reasons for RBC membranes supported endothelialization are as follows: (1) high expression of CD47 protein on the surface of RBC membrane plays important roles in promoting HUVECs' adhesion, proliferation, and migration;[58,59] and (2) the biomimetic nanoparticles modified heart valves exhibited good biocompatibility to HUVECs compared with the GLU-treated valves.

https://dx.doi.org/10.1021/acsami.0c12688
ACS Appl. Mater. Interfaces 2020, 12, 41113−41126

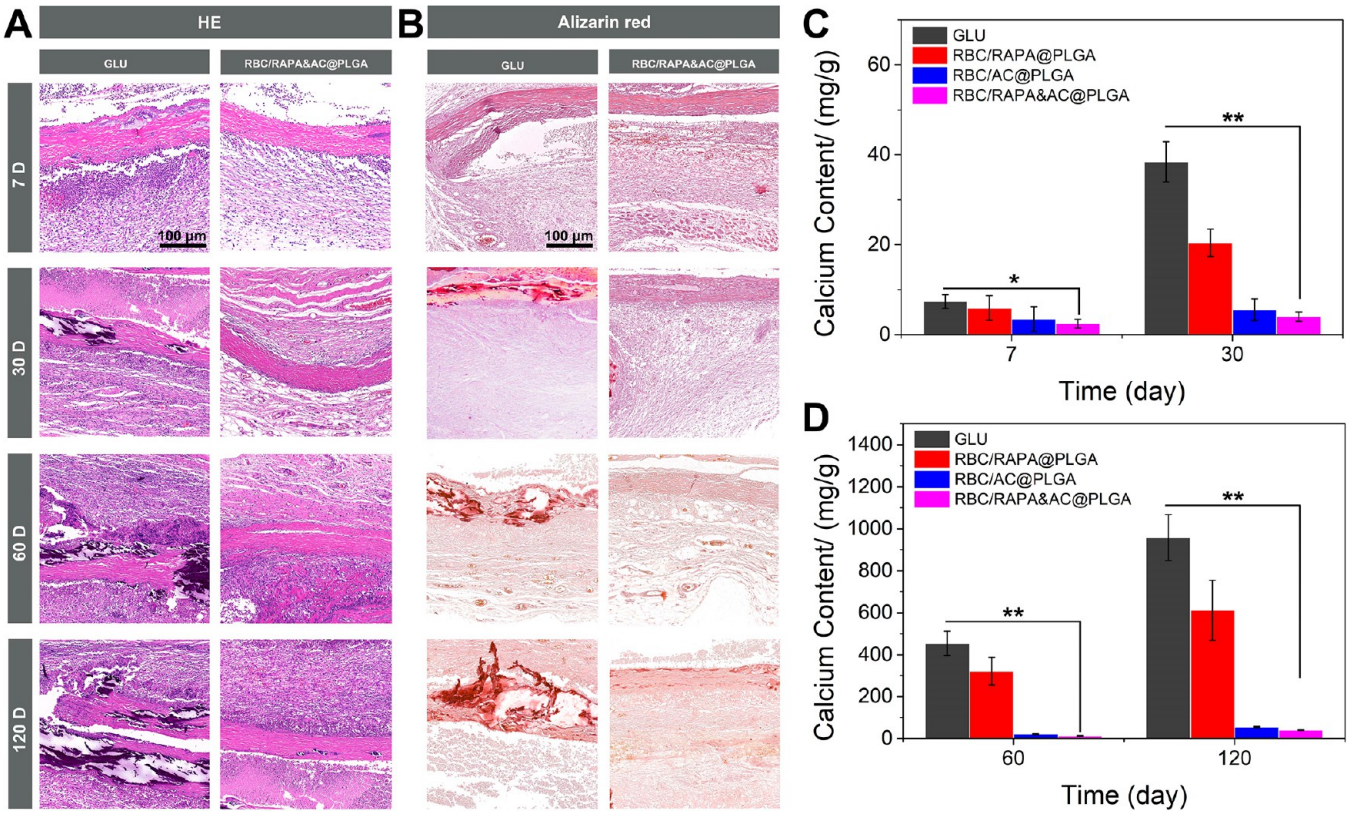

Figure 5. (A) HE staining of different heart valves at 7, 30, 60, and 120 days postimplantation into male SD rats. (B) Alizarin red staining of different heart valves at 7, 30, 60, and 120 days postimplantation into male SD rats. All scale bars = 100 μm. (C) Calcium contents of different heart valves at 7 and 30 days were calculated (mean ± SD; n = 6; *, $P < 0.01$; **, $P < 0.001$). (D) Calculated calcium contents of different heart valves at 60 and 120 days (mean ± SD; n = 6; **,$P < 0.001$).

Macrophage inflammation plays a significant effect in the calcification of the heart valves.[60] And the macrophages could be preactivated with LPS (lipopolysaccharide) to mimic the inflammatory environment and create a first-rank inflammatory environment to expound the efficacy of drug-loaded nanoparticle-modified valves in inhibiting inflammation.[61] First, the cell viability results of raw 246.7 cells in Figure 4A indicated that the RBC/RAPA&AC@PLGA group enhanced the survival rate of macrophages which were preactivated with LPS at days 1 and 3. This is mainly due to the AC drug released from the RBC/RAPA&AC@PLGA nanoparticles reducing the inflammatory response of macrophages. However, GLU group heart valves further decreased the survival rate of macrophages, mainly due to their own cytotoxicity and inability to suppress inflammation response. Interleukin-10 is a potent pleiotropic cytokine with anti-inflammatory properties, however, TNF-α pathway plays a pivotal pro-inflammatory role in inflammatory diseases.[62] IL-10 and TNF-α expression were quantified by ELISA. The quantitative analysis results in Figure 4B,C suggested that the expression level of IL-10 in the RBC/RAPA&AC@PLGA group enhanced 230% and the expression level of TNF-α reduced 69% compared with that of the GLU group. Western blot assays were also utilized to evaluate the expression levels of inflammatory-related proteins. As shown in Figure 4D, the RBC/RAPA&AC@PLGA group could enhance the expression of IL-10 and decrease the expression of TNF-α compared with that in the GLU group. Finally, IL-10 and TNF-α were measured by immunofluorescence staining. For IL-10 immunofluorescence staining, the green fluorescence in the RBC/RAPA&AC@PLGA group was higher than that in the GLU group. The results in Figure 4E suggested that the RBC/RAPA&AC@PLGA group increased the expression of IL-10 in LPS-activated macrophages. However, the weaker green fluorescence in the RBC/RAPA&AC@PLGA group than the GLU group indicated that the expression of TNF-α was decreased (Figure 4F). Immunofluorescence staining results suggested that RBC/RAPA&AC@PLGA group could reduce inflammation response in LPS-activated macrophages.

To study the effects of heart valves after being modified with the RBC coated drug-loaded nanoparticles *in vivo*, different heart valve samples were subcutaneously implanted in male Sprague−Dawley (SD) rats for 7, 30, 60, and 120 days to examine the biocompatibility *in vivo*.[19] The H&E of tissue sections (Figure 5A and Figure S15) showed that the GLU group had significant abnormal damage and many loose regions in the pericardium−tissue interface compared with the RBC/RAPA&AC@PLGA group at 120 days. The results also revealed that the RBC/RAPA&AC@PLGA group had better biocompatibility *in vivo* than the GLU group. To assess the calcification after valves implantation, an alizarin red staining experiment was carried out.[63] As shown in Figure 5B and Figure S15, alizarin red staining of the RBC/RAPA&AC@PLGA group showed few calcification deposits, while the GLU control group manifested many more at 120 days. Calcium content was quantified by inductively coupled plasma optical emission spectrometer (ICP-OES;[64] Figure 5C,D); the calcium content of the GLU control group significantly increased with the time of implantation. The calcium content increased from 38.4 mg/g tissue dry weight at 30 days to 957.9

https://dx.doi.org/10.1021/acsami.0c12688
ACS Appl. Mater. Interfaces 2020, 12, 41113−41126

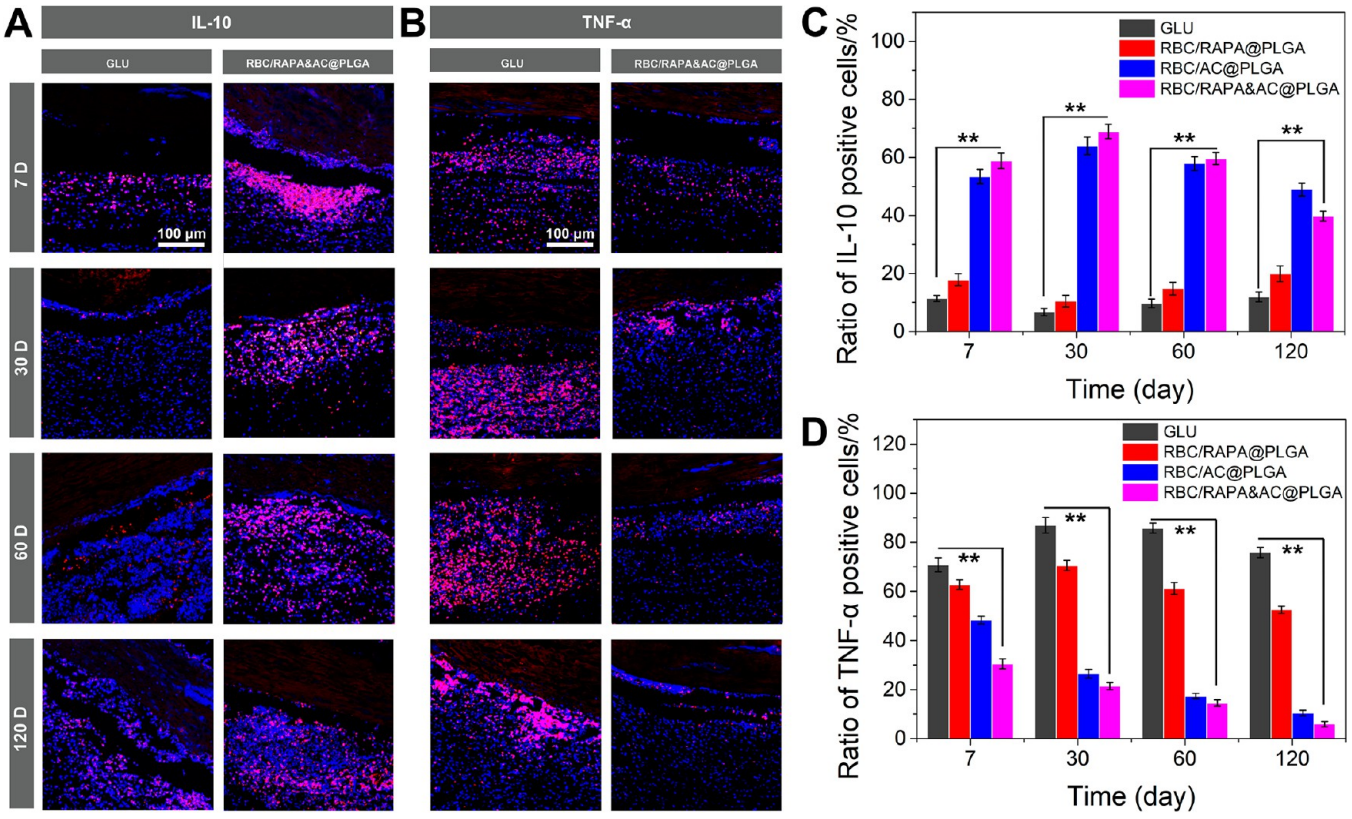

Figure 6. (A) IL-10 and (B) TNF-α of different heart valves at 7, 30, 60, and 120 days postimplantation into male SD rats. All scale bars = 100 μm. (C) Ratio of IL-10 positive cells at 7, 30, 60, and 120 days (mean ± SD; n = 6; **,P < 0.001). (D) Ratio of TNF-α positive cells at 7, 30, 60, and 120 days (mean ± SD; n = 6; **,P < 0.001).

mg/g tissue dry weight at 120 days. However, the calcium content of the RBC/RAPA&AC@PLGA group had only a modest increase in tissue dry weight from 4.0 mg/g at 30 days to 39.7 mg/g at 120 days. The calcium content in the RBC/RAPA&AC@PLGA group was always conspicuously lower than that in the GLU group at detective time points. This demonstrated that the RBC/RAPA&AC@PLGA group has the least calcification compared to other groups. In summary, the results suggested that the nanoparticle modification strategy had the potential for anti-calcification of heart valves.

Calcification of biological heart valves is known to be associated with inflammation response *in vivo*.[65] Accordingly, we further studied the inflammation response after valves implantation in the rat.[23] Here, TNF-α and IL-10 were selected as indicators to assess the inflammation *in vivo*. The IL-10 staining results in Figure 6A and Figure S16 showed higher levels of IL-10 in the RBC/RAPA&AC@PLGA group at multiple time points (7, 30, 60, and 120 days) than those in GLU group. Quantification in Figure 6C revealed that there was a 68.8% IL-10-positive cell ratio after 30 days of implantation in the RBC/RAPA&AC@PLGA group, which represented a greater increase compared to that of the GLU group (6.7% in IL-10-positive cell ratio), indicating severe inflammation in the GLU group. At 120 days, the ratios of IL-10-positive cells in the RBC/RAPA&AC@PLGA and GLU groups were 39.8% and 11.9%, respectively. The results in Figure 6B and Figure S16 also indicated lower numbers of TNF-α-positive cells at 7, 30, 60, and 120 days in the RBC/RAPA&AC@PLGA group compared to the GLU control group. The results were consistent with those in Figure 6D. The number of TNF-α-positive cells comparatively decreased after 30 days with implantations compared with those at 7 days (from 30.5% to 21.4%), suggesting that the inflammation response was reduced in the RBC/RAPA&AC@PLGA group. The RBC/RAPA&AC@PLGA group (5.9%) had a lower positive cell ratio at 120 days than the GLU control group (75.8%), indicating that the RBC/RAPA&AC@PLGA group induced a milder inflammation response than GLU group due to the release of the anti-inflammatory drug AC. Interestingly, in the GLU group, we found that the TNF-α-positive cell rate was slightly reduced at 120 days after implantation compared to 60 days (from 85.7% to 75.8%); we speculated that this might be related to the immune regulation system of the rats themselves. In conclusion, these results indicated that the RBC/RAPA&AC@PLGA group could more effectively decrease the inflammation response than the GLU group after valves implantation in the rat.

4. CONCLUSION

In summary, we developed a new cross-linking-modified strategy for combining a biomimetic drug delivery system with biological heart valves that effectively overcomes its existing problems in clinical application. To the best of our knowledge, this concept and design strategy has not been reported. The heart valves that were cross-linked with the RBC/RAPA&AC@PLGA nanoparticles preserved the structural stability and mechanical properties of the GLU-treated heart valves. Most importantly, the heart valves modified with biomimetic drug-loaded nanoparticles exhibited excellent biological performance. First, we reported that the novel heart valves have more long-term anti-coagulation properties

https://dx.doi.org/10.1021/acsami.0c12688
ACS Appl. Mater. Interfaces 2020, 12, 41113−41126

and better blood compatibility than the GLU-treated heart valves. Second, the modification of the RBC-coated drug-loaded nanoparticles provide a potential function in promoting the heart valve endothelialization process. Lastly, the modified heart valves have ultrastrong resistance to calcification after implantation in rats, for at least 120 days. Through *in vitro* and *in vivo* experiments, we also elucidated the mechanism of anti-calcification after valve implantation as mainly being due to the rapid endothelialization and controlled release of anti-inflammatory drugs to reduce the inflammatory response. In summary, the *in vitro* and *in vivo* data confirmed the use of novel heart valves that were cross-linked with erythrocyte membrane, biomimetic drug-loaded nanoparticles as an effective method for anti-coagulation, endothelialization, and anti-calcification *via* inhibition of the inflammatory response. Our strategy offers a valid modality for ameliorating heart valves and opens a new window into exploiting biomimetic nanomaterials to overcome the shortcomings of biological heart valves. Most importantly, our heart valve modification strategy holds great potential for clinical translation.

■ ASSOCIATED CONTENT

Supporting Information

The Supporting Information is available free of charge at https://pubs.acs.org/doi/10.1021/acsami.0c12688.

Additional graphs; particle size distribution and ζ potential of nanoparticles; glycoprotein content; SEM images; nanoparticle content; ATR-FTIR spectra; fluorescence intensity of DiD@PLGA nanoparticles; representative stress−strain curves of heart valves; cell viability; concentrations of C3a; HE and alizarin red staining; IL-10 and TNF-α data (PDF)

■ AUTHOR INFORMATION

Corresponding Author

Yunbing Wang − *National Engineering Research Center for Biomaterials, Sichuan University, Chengdu, Sichuan 610064, People's Republic of China;* orcid.org/0000-0002-2412-6762; Phone: +86-28-85410280; Email: yunbing.wang@scu.edu.cn

Authors

Cheng Hu − *National Engineering Research Center for Biomaterials, Sichuan University, Chengdu, Sichuan 610064, People's Republic of China;* orcid.org/0000-0003-4316-231X

Rifang Luo − *National Engineering Research Center for Biomaterials, Sichuan University, Chengdu, Sichuan 610064, People's Republic of China;* orcid.org/0000-0002-8998-9948

Complete contact information is available at: https://pubs.acs.org/10.1021/acsami.0c12688

Notes

The authors declare no competing financial interest.

■ ACKNOWLEDGMENTS

This work was supported by the funding listed as follows: Interdisciplinary innovation cultivation project of Sichuan University (Grant No. 0900904153015), the National Natural Science Foundation of China (Grant No. 51703144), China Postdoctoral Science Foundation (Grant No. 2018T110976), the 111 Project (The Program of Introducing Talents of Discipline to Universities (Grant No. B16033)), and Sichuan Science and Technology Major Project (Grant No. 2018SZDZX0011). We thank "ceshigo" (http://www.ceshigo.com/) for ICP-OES testing analysis.

■ REFERENCES

(1) Nkomo, V. T.; Gardin, J. M.; Skelton, T. N.; Gottdiener, J. S.; Scott, C. G.; Enriquez-Sarano, M. Burden of Valvular Heart Diseases: A Population-Based Study. *Lancet* **2006**, *368* (9540), 1005−1011.

(2) Iung, B.; Vahanian, A. Epidemiology of Valvular Heart Disease in the Adult. *Nat. Rev. Cardiol.* **2011**, *8* (3), 162−172.

(3) Maganti, K.; Rigolin, V. H.; Sarano, M. E.; Bonow, R. O. Valvular Heart Disease: Diagnosis and Management. *Mayo Clin. Proc.* **2010**, *85* (5), 483−500.

(4) Rahimtoola, S. H. Valvular Heart Disease: A Perspective. *J. Am. Coll. Cardiol.* **1983**, *1* (1), 199−215.

(5) Dunning, J.; Gao, H.; Chambers, J.; Moat, N.; Murphy, G.; Pagano, D.; Ray, S.; Roxburgh, J.; Bridgewater, B. Aortic Valve Surgery: Marked Increases in Volume and Significant Decreases in Mechanical Valve Use-An Analysis of 41,227 Patients over 5 Years from the Society for Cardiothoracic Surgery in Great Britain and Ireland National Database. *J. Thorac. Cardiovasc. Surg.* **2011**, *142* (4), 776−782.e3.

(6) Fioretta, E. S.; Dijkman, P. E.; Emmert, M. Y.; Hoerstrup, S. P. The Future of Heart Valve Replacement: Recent Developments and Translational Challenges for Heart Valve Tissue Engineering. *J. Tissue Eng. Regener. Med.* **2018**, *12* (1), e323−e335.

(7) Yacoub, M.; Takkenberg, J. Will Heart Valve Tissue Engineering Change the World? Nat Clin Pract Cardiovasc Med. *Nat. Clin. Pract. Cardiovasc. Med.* **2005**, *2*, 60−1.

(8) Gales, J.; Krasuski, R. A.; Fleming, G. A. Transcatheter Valve Replacement for Right-Sided Valve Disease in Congenital Heart Patients. *Prog. Cardiovasc. Dis.* **2018**, *61* (3), 347−359.

(9) Jin, L.; Guo, G.; Jin, W.; Lei, Y.; Wang, Y. Cross-Linking Methacrylated Porcine Pericardium by Radical Polymerization Confers Enhanced Extracellular Matrix Stability, Reduced Calcification, and Mitigated Immune Response to Bioprosthetic Heart Valves. *ACS Biomater. Sci. Eng.* **2019**, *5* (4), 1822−1832.

(10) Cheung, A.; Webb, J.; Schaefer, U.; Moss, R.; Deuschl, F. G.; Conradi, L.; Denti, P.; Latib, A.; Kiaii, B.; Bagur, R.; Ferrari, E.; Moccetti, M.; Biasco, L.; Blanke, P.; Ben-Gal, Y.; Banai, S. Transcatheter Mitral Valve Replacement in Patients with Previous Aortic Valve Replacement. *Circ.: Cardiovasc. Interventions* **2018**, *11* (10), e006412.

(11) Issa, I. F.; Dahl, J. S.; Poulsen, S. H.; Waziri, F.; Pedersen, C. T.; Riber, L.; Søgaard, P.; Møller, J. E. The Relation of Structural Valve Deterioration to Adverse Remodelling and Outcome in Patients with Biological Heart Valve Prostheses. *Eur. Heart J.: Cardiovasc. Imag.* **2020**, jez317.

(12) Neuenschwander, S.; Hoerstrup, S. P. Heart Valve Tissue Engineering. *Transplant Immunol.* **2004**, *12* (3), 359−365.

(13) Hofferberth, S. C.; Saeed, M. Y.; Tomholt, L.; Fernandes, M. C.; Payne, C. J.; Price, K.; Marx, G. R.; Esch, J. J.; Brown, D. W.; Brown, J.; Hammer, P. E.; Bianco, R. W.; Weaver, J. C.; Edelman, E. R.; del Nido, P. J. A Geometrically Adaptable Heart Valve Replacement. *Sci. Transl. Med.* **2020**, *12* (531), eaay4006.

(14) Chakravarty, T.; Søndergaard, L.; Friedman, J.; De Backer, O.; Berman, D.; Kofoed, K. F.; Jilaihawi, H.; Shiota, T.; Abramowitz, Y.; Jørgensen, T. H.; Rami, T.; Israr, S.; Fontana, G.; de Knegt, M.; Fuchs, A.; Lyden, P.; Trento, A.; Bhatt, D. L.; Leon, M. B.; Makkar, R. R.; Ramzy, D.; Cheng, W.; Siegel, R. J.; Thomson, L. M.; Mangat, G.; Hariri, B.; Sawaya, F. J.; Iversen, H. K. Subclinical Leaflet Thrombosis in Surgical and Transcatheter Bioprosthetic Aortic Valves: An Observational Study. *Lancet* **2017**, *389* (10087), 2383−2392.

(15) Nakatani, S. Subclinical Leaflet Thrombosis after Transcatheter Aortic Valve Implantation. *Heart* **2017**, *103* (24), 1942−1946.

(16) Del Trigo, M.; Muñoz-García, A. J.; Latib, A.; Auffret, V.; Wijeysundera, H. C.; Nombela-Franco, L.; Gutierrez, E.; Cheema, A. N.; Serra, V.; Amat-Santos, I. J.; Kefer, J.; Benitez, L. M.; Leclercq, F.; Mangieri, A.; Le Breton, H.; Jiménez-Quevedo, P.; Garcia del Blanco, B.; Dager, A.; Abdul-Jawad Altisent, O.; Puri, R.; Pibarot, P.; Rodés-Cabau, J. Impact of Anticoagulation Therapy on Valve Haemodynamic Deterioration Following Transcatheter Aortic Valve Replacement. *Heart* **2018**, *104* (10), 814.
(17) Doris, M. K.; Dweck, M. R. Is Bioprosthetic Leaflet Thrombosis a Trigger to Valve Degeneration? *Heart* **2018**, *104* (10), 792.
(18) Wolberg, A. S.; Aleman, M. M.; Leiderman, K.; Machlus, K. R. Procoagulant Activity in Hemostasis and Thrombosis: Virchow's Triad Revisited. *Anesth. Analg.* **2012**, *114* (2), 275−285.
(19) Yang, L.; Huang, X.; Deng, L.; Ma, X.; Jiang, H.; Ning, Q.; Liang, Z.; Lei, Y.; Wang, Y. Pre-Mounted Dry Tavi Valve with Improved Endothelialization Potential Using Redv-Loaded Pegma Hydrogel Hybrid Pericardium. *J. Mater. Chem. B* **2020**, *8* (13), 2689−2701.
(20) Lopez-Moya, M.; Melgar-Lesmes, P.; Kolandaivelu, K.; de la Torre Hernández, J. M.; Edelman, E. R.; Balcells, M. Optimizing Glutaraldehyde-Fixed Tissue Heart Valves with Chondroitin Sulfate Hydrogel for Endothelialization and Shielding against Deterioration. *Biomacromolecules* **2018**, *19* (4), 1234−1244.
(21) Guo, G.; Jin, W.; Jin, L.; Chen, L.; Lei, Y.; Wang, Y. Hydrogel Hybrid Porcine Pericardium for the Fabrication of a Pre-Mounted Tavi Valve with Improved Biocompatibility. *J. Mater. Chem. B* **2019**, *7* (9), 1427−1434.
(22) Tam, H.; Zhang, W.; Feaver, K. R.; Parchment, N.; Sacks, M. S.; Vyavahare, N. A Novel Crosslinking Method for Improved Tear Resistance And biocompatibility of Tissue Based Biomaterials. *Biomaterials* **2015**, *66*, 83−91.
(23) Guo, F.; Liu, Y.; Jiao, K.; Yang, R.; Hou, M.; Zhang, X. Artificial Heart Valves with Balanced Charged Networks Exhibiting Anti-Calcification Properties. *ACS Applied Bio Materials* **2020**, *3* (2), 838−847.
(24) Guo, G.; Jin, L.; Jin, W.; Chen, L.; Lei, Y.; Wang, Y. Radical Polymerization-Crosslinking Method for Improving Extracellular Matrix Stability in Bioprosthetic Heart Valves with Reduced Potential for Calcification and Inflammatory Response. *Acta Biomater.* **2018**, *82*, 44−55.
(25) Li, M.; Ning, Y.; Chen, J.; Duan, X.; Song, N.; Ding, D.; Su, X.; Yu, Z. Proline Isomerization-Regulated Tumor Microenvironment-Adaptable Self-Assembly of Peptides for Enhanced Therapeutic Efficacy. *Nano Lett.* **2019**, *19* (11), 7965−7976.
(26) Lin, A.; Liu, Y.; Zhu, X.; Chen, X.; Liu, J.; Zhou, Y.; Qin, X.; Liu, J. Bacteria-Responsive Biomimetic Selenium Nanosystem for Multidrug-Resistant Bacterial Infection Detection and Inhibition. *ACS Nano* **2019**, *13* (12), 13965−13984.
(27) Yang, H.; Qin, X.; Wang, H.; Zhao, X.; Liu, Y.; Wo, H.-T.; Liu, C.; Nishiga, M.; Chen, H.; Ge, J.; Sayed, N.; Abilez, O. J.; Ding, D.; Heilshorn, S. C.; Li, K. An in Vivo Mirna Delivery System for Restoring Infarcted Myocardium. *ACS Nano* **2019**, *13* (9), 9880−9894.
(28) Park, J. H.; Dehaini, D.; Zhou, J.; Holay, M.; Fang, R. H.; Zhang, L. Biomimetic Nanoparticle Technology for Cardiovascular Disease Detection and Treatment. *Nanoscale Horizons* **2020**, *5* (1), 25−42.
(29) Majumder, J.; Taratula, O.; Minko, T. Nanocarrier-Based Systems for Targeted and Site Specific Therapeutic Delivery. *Adv. Drug Delivery Rev.* **2019**, *144*, 57−77.
(30) Zhang, W.; Wang, M.; Tang, W.; Wen, R.; Zhou, S.; Lee, C.; Wang, H.; Jiang, W.; Delahunty, I. M.; Zhen, Z.; Chen, H.; Chapman, M.; Wu, Z.; Howerth, E. W.; Cai, H.; Li, Z.; Xie, J. Nanoparticle-Laden Macrophages for Tumor-Tropic Drug Delivery. *Adv. Mater.* **2018**, *30* (50), 1805557.
(31) Han, Y.; Pan, H.; Li, W.; Chen, Z.; Ma, A.; Yin, T.; Liang, R.; Chen, F.; Ma, Y.; Jin, Y.; Zheng, M.; Li, B.; Cai, L. T Cell Membrane Mimicking Nanoparticles with Bioorthogonal Targeting and Immune Recognition for Enhanced Photothermal Therapy. *Advanced Science* **2019**, *6* (15), 1900251.
(32) Dong, X.; Gao, J.; Zhang, C. Y.; Hayworth, C.; Frank, M.; Wang, Z. Neutrophil Membrane-Derived Nanovesicles Alleviate Inflammation to Protect Mouse Brain Injury from Ischemic Stroke. *ACS Nano* **2019**, *13* (2), 1272−1283.
(33) Cheng, H.; Byrska-Bishop, M.; Zhang, C. T.; Kastrup, C. J.; Hwang, N. S.; Tai, A. K.; Lee, W. W.; Xu, X.; Nahrendorf, M.; Langer, R.; Anderson, D. G. Stem Cell Membrane Engineering for Cell Rolling Using Peptide Conjugation and Tuning of Cell−Selectin Interaction Kinetics. *Biomaterials* **2012**, *33* (20), 5004−5012.
(34) Wang, Y.; Zhang, K.; Qin, X.; Li, T.; Qiu, J.; Yin, T.; Huang, J.; McGinty, S.; Pontrelli, G.; Ren, J.; Wang, Q.; Wu, W.; Wang, G. Biomimetic Nanotherapies: Red Blood Cell Based Core−Shell Structured Nanocomplexes for Atherosclerosis Management. *Advanced Science* **2019**, *6* (12), 1900172.
(35) Song, Y.; Huang, Z.; Liu, X.; Pang, Z.; Chen, J.; Yang, H.; Zhang, N.; Cao, Z.; Liu, M.; Cao, J.; Li, C.; Yang, X.; Gong, H.; Qian, J.; Ge, J. Platelet Membrane-Coated Nanoparticle-Mediated Targeting Delivery of Rapamycin Blocks Atherosclerotic Plaque Development and Stabilizes Plaque in Apolipoprotein E-Deficient (Apoe−/−) Mice. *Nanomedicine* **2019**, *15* (1), 13−24.
(36) Fang, R. H.; Kroll, A. V.; Gao, W.; Zhang, L. Cell Membrane Coating Nanotechnology. *Adv. Mater.* **2018**, *30* (23), 1706759.
(37) Chen, Z.; Wang, Z.; Gu, Z. Bioinspired and Biomimetic Nanomedicines. *Acc. Chem. Res.* **2019**, *52* (5), 1255−1264.
(38) Zhang, P.; Liu, G.; Chen, X. Nanobiotechnology: Cell Membrane-Based Delivery Systems. *Nano Today* **2017**, *13*, 7−9.
(39) Chai, Z.; Ran, D.; Lu, L.; Zhan, C.; Ruan, H.; Hu, X.; Xie, C.; Jiang, K.; Li, J.; Zhou, J.; Wang, J.; Zhang, Y.; Fang, R. H.; Zhang, L.; Lu, W. Ligand-Modified Cell Membrane Enables the Targeted Delivery of Drug Nanocrystals to Glioma. *ACS Nano* **2019**, *13* (5), 5591−5601.
(40) Yang, J.; Wang, F.; Lu, Y.; Qi, J.; Deng, L.; Sousa, F.; Sarmento, B.; Xu, X.; Cui, W. Recent Advance of Erythrocyte-Mimicking Nanovehicles: From Bench to Bedside. *J. Controlled Release* **2019**, *314*, 81−91.
(41) Visner, G. A.; Lu, F.; Zhou, H.; Liu, J.; Kazemfar, K.; Agarwal, A. Rapamycin Induces Heme Oxygenase-1 in Human Pulmonary Vascular Cells. *Circulation* **2003**, *107* (6), 911−916.
(42) Schwinté, P.; Mariotte, A.; Anand, P.; Keller, L.; Idoux-Gillet, Y.; Huck, O.; Fioretti, F.; Tenenbaum, H.; Georgel, P.; Wenzel, W.; Irusta, S.; Benkirane-Jessel, N. Anti-Inflammatory Effect of Active Nanofibrous Polymeric Membrane Bearing Nanocontainers of Atorvastatin Complexes. *Nanomedicine* **2017**, *12* (23), 2651−2674.
(43) Swider, E.; Koshkina, O.; Tel, J.; Cruz, L. J.; de Vries, I. J. M.; Srinivas, M. Customizing Poly(Lactic-Co-Glycolic Acid) Particles for Biomedical Applications. *Acta Biomater.* **2018**, *73*, 38−51.
(44) Tziakas, D. N.; Chalikias, G.; Pavlaki, M.; Kareli, D.; Gogiraju, R.; Hubert, A.; Böhm, E.; Stamoulis, P.; Drosos, I.; Kikas, P.; Mikroulis, D.; Giatromanolaki, A.; Georgiadis, G. S.; Konstantinou, F.; Argyriou, C.; Münzel, T.; Konstantinides, S. V.; Schäfer, K. Lysed Erythrocyte Membranes Promote Vascular Calcification. *Circulation* **2019**, *139* (17), 2032−2048.
(45) Hu, C.; Zhang, F.; Long, L.; Kong, Q.; Luo, R.; Wang, Y. Dual-Responsive Injectable Hydrogels Encapsulating Drug-Loaded Micelles for on-Demand Antimicrobial Activity and Accelerated Wound Healing. *J. Controlled Release* **2020**, *324*, 204.
(46) Hu, C.; Zhang, F.; Kong, Q.; Lu, Y.; Zhang, B.; Wu, C.; Luo, R.; Wang, Y. Synergistic Chemical and Photodynamic Antimicrobial Therapy for Enhanced Wound Healing Mediated by Multifunctional Light-Responsive Nanoparticles. *Biomacromolecules* **2019**, *20* (12), 4581−4592.
(47) Jiang, Y.; Krishnan, N.; Zhou, J.; Chekuri, S.; Wei, X.; Kroll, A. V.; Yu, C. L.; Duan, Y.; Gao, W.; Fang, R. H.; Zhang, L. Engineered Cell-Membrane-Coated Nanoparticles Directly Present Tumor Antigens to Promote Anticancer Immunity. *Adv. Mater.* **2020**, *32* (30), 2001808.

https://dx.doi.org/10.1021/acsami.0c12688
ACS Appl. Mater. Interfaces 2020, 12, 41113−41126

(48) Oldenborg, P.-A.; Zheleznyak, A.; Fang, Y.-F.; Lagenaur, C. F.; Gresham, H. D.; Lindberg, F. P. Role of Cd47 as a Marker of Self on Red Blood Cells. *Science* **2000**, *288* (5473), 2051.
(49) Hu, C.-M. J.; Zhang, L.; Aryal, S.; Cheung, C.; Fang, R. H.; Zhang, L. Erythrocyte Membrane-Camouflaged Polymeric Nanoparticles as a Biomimetic Delivery Platform. *Proc. Natl. Acad. Sci. U. S. A.* **2011**, *108* (27), 10980.
(50) Zhou, J.; Ding, J.; Zhu, Z.; Xu, J.; Yi, Y.; Li, Y.; Fan, H.; Bai, S.; Yang, J.; Tang, Y.; Dong, X.; Dong, N. Surface Biofunctionalization of the Decellularized Porcine Aortic Valve with Vegf-Loaded Nanoparticles for Accelerating Endothelialization. *Mater. Sci. Eng., C* **2019**, *97*, 632−643.
(51) Lu, J.; Zhuang, W.; Li, L.; Zhang, B.; Yang, L.; Liu, D.; Yu, H.; Luo, R.; Wang, Y. Micelle-Embedded Layer-by-Layer Coating with Catechol and Phenylboronic Acid for Tunable Drug Loading, Sustained Release, Mild Tissue Response, and Selective Cell Fate for Re-Endothelialization. *ACS Appl. Mater. Interfaces* **2019**, *11* (10), 10337−10350.
(52) Moghimi, S. M.; Simberg, D. Complement Activation Turnover on Surfaces of Nanoparticles. *Nano Today* **2017**, *15*, 8−10.
(53) McGregor, C.; Byrne, G.; Rahmani, B.; Chisari, E.; Kyriakopoulou, K.; Burriesci, G. Physical Equivalency of Wild Type and Galactose A 1,3 Galactose Free Porcine Pericardium; a New Source Material for Bioprosthetic Heart Valves. *Acta Biomater.* **2016**, *41*, 204−209.
(54) Zhang, R.; Wang, Y.; Chen, L.; Wang, R.; Li, C.; Li, X.; Fang, B.; Ren, X.; Ruan, M.; Liu, J.; Xiong, Q.; Zhang, L.; Jin, Y.; Zhang, M.; Liu, X.; Li, L.; Chen, Q.; Pan, D.; Li, R.; Cooper, D. K. C.; Yang, H.; Dai, Y. Reducing Immunoreactivity of Porcine Bioprosthetic Heart Valves by Genetically-Deleting Three Major Glycan Antigens, Ggta1/B4galnt2/Cmah. *Acta Biomater.* **2018**, *72*, 196−205.
(55) McGregor, C. G. A.; Carpentier, A.; Lila, N.; Logan, J. S.; Byrne, G. W. Cardiac Xenotransplantation Technology Provides Materials for Improved Bioprosthetic Heart Valves. *J. Thorac. Cardiovasc. Surg.* **2011**, *141* (1), 269−275.
(56) Shi, Q.; Fan, Q.; Ye, W.; Hou, J.; Wong, S.-C.; Xu, X.; Yin, J. Controlled Lecithin Release from a Hierarchical Architecture on Blood-Contacting Surface to Reduce Hemolysis of Stored Red Blood Cells. *ACS Appl. Mater. Interfaces* **2014**, *6* (12), 9808−9814.
(57) Yildirim, A.; Demirel, G. B.; Erdem, R.; Senturk, B.; Tekinay, T.; Bayindir, M. Pluronic Polymer Capped Biocompatible Mesoporous Silica Nanocarriers. *Chem. Commun.* **2013**, *49* (84), 9782−9784.
(58) Reed, M.; Luissint, A.-C.; Azcutia, V.; Fan, S.; O'Leary, M. N.; Quiros, M.; Brazil, J.; Nusrat, A.; Parkos, C. A. Epithelial Cd47 Is Critical for Mucosal Repair in the Murine Intestine in Vivo. *Nat. Commun.* **2019**, *10* (1), 5004.
(59) Inamdar, V. V.; Fitzpatrick, E.; Alferiev, I.; Nagaswami, C.; Spruce, L. A.; Fazelinia, H.; Bratinov, G.; Seeholzer, S. H.; Levy, R. J.; Fishbein, I.; Stachelek, S. J. Stability and Bioactivity of Pepcd47 Attachment on Stainless Steel Surfaces. *Acta Biomater.* **2020**, *104*, 231−240.
(60) Manji, R. A.; Zhu, L. F.; Nijjar, N. K.; Rayner, D. C.; Korbutt, G. S.; Churchill, T. A.; Rajotte, R. V.; Koshal, A.; Ross, D. B. Glutaraldehyde-Fixed Bioprosthetic Heart Valve Conduits Calcify and Fail from Xenograft Rejection. *Circulation* **2006**, *114* (4), 318−327.
(61) Hardy, A.; Seguin, C.; Brion, A.; Lavalle, P.; Schaaf, P.; Fournel, S.; Bourel-Bonnet, L.; Frisch, B.; De Giorgi, M. B-Cyclodextrin-Functionalized Chitosan/Alginate Compact Polyelectrolyte Complexes (Copecs) as Functional Biomaterials with Anti-Inflammatory Properties. *ACS Appl. Mater. Interfaces* **2018**, *10* (35), 29347−29356.
(62) Hu, C.; Zhang, F.; Long, L.; Kong, Q.; Luo, R.; Wang, Y. Dual-Responsive Injectable Hydrogels Encapsulating Drug-Loaded Micelles for on-Demand Antimicrobial Activity and Accelerated Wound Healing. *J. Controlled Release* **2020**, *324*, 204−217.
(63) Osako, M. K.; Nakagami, H.; Koibuchi, N.; Shimizu, H.; Nakagami, F.; Koriyama, H.; Shimamura, M.; Miyake, T.; Rakugi, H.; Morishita, R. Estrogen Inhibits Vascular Calcification Via Vascular RANKL System. *Circ. Res.* **2010**, *107* (4), 466−475.
(64) Liu, J.; Jing, H.; Qin, Y.; Li, B.; Sun, Z.; Kong, D.; Leng, X.; Wang, Z. Nonglutaraldehyde Fixation for Off the Shelf Decellularized Bovine Pericardium in Anticalcification Cardiac Valve Applications. *ACS Biomater. Sci. Eng.* **2019**, *5* (3), 1452−1461.
(65) Huk, D. J.; Hammond, H. L.; Kegechika, H.; Lincoln, J. Increased Dietary Intake of Vitamin A Promotes Aortic Valve Calcification in Vivo. *Arterioscler., Thromb., Vasc. Biol.* **2013**, *33* (2), 285−293.

https://dx.doi.org/10.1021/acsami.0c12688
ACS Appl. Mater. Interfaces 2020, 12, 41113−41126